Available online at www.sciencedirect.com
ScienceDirect
Journal of Solid State Chemistry 180 (2007) 3280–3287
JOURNAL OF SOLID STATE CHEMISTRY
www.elsevier.com/locate/jssc

Ab initio study on structure and phase transition of *A*- and *B*-type rare-earth sesquioxides Ln_2O_3 (*Ln* = La–Lu, Y, and Sc) based on density function theory

Bo Wu[a,b,*], Matvei Zinkevich[b], Fritz Aldinger[b], Dingzhong Wen[a], Lu Chen[a]

[a]*College of Materials Science and Engineering, Fuzhou University, University Park, 350108 Fuzhou, PR China*
[b]*Max-Planck-Institut für Metallforschung und Institut für Nichtmetallische Anorganische Materialien der Universität Stuttgart, Heisenbergstrasse 3, 70569 Stuttgart, Germany*

Received 29 July 2007; received in revised form 9 September 2007; accepted 15 September 2007
Available online 26 September 2007

Abstract

Ab initio energetic calculations based on the density functional theory (DFT) and projector augmented wave (PAW) pseudo-potentials method were performanced to determine the crystal structural parameters and phase transition data of the polymorphic rare-earth sesquioxides Ln_2O_3 (where *Ln* = La–Lu, Y, and Sc) with *A*-type (hexagonal) and *B*-type (monoclinic) configurations at ground state. The calculated results agree well with the limited experimental data and the critically assessed results. A set of systematic and self-consistent crystal structural parameters, energies and pressures of the phase transition were established for the whole series of the *A*- and *B*-type rare-earth sesquioxides Ln_2O_3. With the increase of the atomic number, the ionic radii of rare-earth elements *Ln* and the volumes of the sesquioxides Ln_2O_3 reflect the so-called "lanthanide contraction". With the increase of the Ln^{3+}-cation radius, the bulk modulus of Ln_2O_3 decreases and the polymorphic structures show a degenerative tendency.

Keywords: Rare-earth sesquioxides; *Ab initio* calculation; Crystal structure; Phase transition

1. Introduction

The rare-earth sesquioxides Ln_2O_3 (where *Ln* = La–Lu, Y, and Sc) are of particular importance due to their unique physical and chemical properties. For example, it has been widely used in chemistry engineering [1], materials science [2–4], metallurgical industry [5], and high-tech agriculture [6,7]. For designing and using such materials, the crystallographic data and thermodynamic properties are of considerable significance. Many literatures, including some review articles [8–14], are available, however, debates and short of data hamper us to establish a robust database for the rare-earth sesquioxides. Depending on the temperature, pressure, and the radius of the Ln^{3+}-cation, rare-earth sesquioxides show five polymorphic modifications as *A*-, *B*-, *C*-, *H*-, and *X*-Ln_2O_3. At ambient conditions, hexagonal *A*-type is the stable structure for *Ln* = La–Nd and probably Pm, while Sm_2O_3, Eu_2O_3, and Gd_2O_3 may exist in both monoclinic *B*-type and cubic *C*-type. The *C*-type is the characteristic structure for *Ln* = Tb–Lu, Y, and Sc. The thermodynamic stability of the *C*-type structure for Sm_2O_3, Eu_2O_3, and Gd_2O_3 at low temperatures is still under debate. The *H*- and *X*-Ln_2O_3 exist only at very high temperatures. Pressure can be viewed as another method to control the relative stability of the polymorphic phases besides temperature. With respect to the pressure-induced phase transition of the Ln_2O_3, only very limited literatures are available [15–23]. Most recently, Zinkevich critically reviewed and derived the thermodynamics of rare-earth sesquioxides [24], however, more fundamental data are needed to strengthen and verify the existing database of the rare-earth sesquioxides Ln_2O_3.

*Corresponding author. College of Materials Science and Engineering, Fuzhou University, University Park, 350108 Fuzhou, PR China.
Fax: +86 591 22866537.
E-mail addresses: wubo@fzu.edu.cn (B. Wu), zinkevich@mf.mpg.de (M. Zinkevich), aldinger@mf.mpg.de (F. Aldinger), wendz2000@yahoo.com.cn (D. Wen), cliiverson@sina.com (L. Chen).

0022-4596/$ - see front matter © 2007 Elsevier Inc. All rights reserved.
doi:10.1016/j.jssc.2007.09.022

With the availability of powerful computer, efficient algorithms and robust software packages, the *ab initio* calculations based on the density functional theory (DFT) [25] are important for understanding the properties of condense matters fundamentally. The universal and high-throughput characters of the *ab initio* method make it a cost-effective tool in solid-state physics and materials science [26]. The most accurate and therefore the most computationally intensive techniques are the full-potential methods [27], nevertheless, considering the limited computer resources, the projector augmented wave (PAW) pseudo-potentials method [28,29] is the state-of-the-art in the *ab initio* calculations. Both the local density approximation (LDA) [30] and the generalized gradient approximation (GGA) [31–33] are used extensively to deal with the exchange-correlation potential of electron gas. Due to the complicated crystal and electronic structure, the *ab initio* structural and energetic calculations on oxide ceramics involving rare-earth element are rare [34–39]. Hirosaki et al. [34] performed the calculations for part of the *A*- and *C*-type of Ln_2O_3 using *ab initio* method based on DFT and PAW, however, there was no energetic information presented.

As a part of the work to establish a comprehensive and self-consistent database for the rare-earth sesquioxides Ln_2O_3 which includes the fundamental data of the crystal, thermodynamics, and phase transition, in the present paper, the *ab initio* structural and energetic calculations based on DFT and PAW for the polymorphic rare-earth sesquioxides Ln_2O_3 with *A*- and *B*-type configurations were performed systematically. The crystal structural parameters and the phase transition data of the Ln_2O_3 from the *B*- to *A*-type were obtained, which considerably strengthened the database of the rare-earth sesquioxides Ln_2O_3.

2. Computational method

The crystallographic information of the *A*- and *B*-type of the polymorphic Ln_2O_3 sesquioxides is given in Table 1, and the coordinate polyhedrons of the Ln_2O_3 are shown in Fig. 1. All cations are in seven-fold in the *A*-type structure, and in the *B*-type structure some of cations are surrounded by seven oxygen anions.

All calculations were carried out using the Vienna *Ab-initio* Simulation Package (VASP) [42–45]. The results correspond to the state at absolute zero temperature and without zero-point motion. For the GGA exchange-correlation energy, the Perdew–Burke–Ernzerhof parameterizations (PBE) [32,33,45] were used. The eigenstates were expanded in the plane-wave basis functions, and the ion cores were represented with the PAW pseudo-potentials [28,29]. The standard PAW pseudo-potential of O was used and the O $2s^2 2p^4$ states were treated as fully relaxed valence states. Base on their similarities to the lanthanide, the *d*-block transition metals Sc and Y are always considered as rare-earth elements. The elements *Ln* in the Ln_2O_3 sesquioxides are normally assumed to be in a trivalent state. As electropositive trivalent metals, all have a closely related chemistry [46]. But their parameterized pseudo-potentials are slightly different due to the different electronic structure. For the *d*-block transition metals, Sc

Table 1
Crystallographic data of the polymorphic Ln_2O_3 sesquioxides

Compound	Structure	Prototype	Pearson symbol	Space group	Number	Strukturbericht Designation	Reference
A-Ln_2O_3	Hexagonal	La_2O_3	hP5	$P\bar{3}m1$	164	$D5_2$	[40]
B-Ln_2O_3	Monoclinic	Sm_2O_3	MC30	$C2/m$	12		[41]

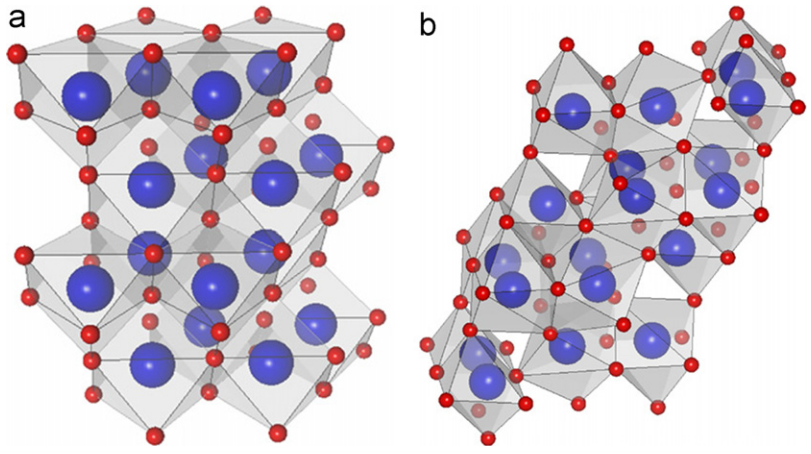

Fig. 1. The coordinate polyhedron of the Ln_2O_3: (a) the hexagonal *A*-type structure; and (b) the monoclinic *B*-type structure. The large and small spheres stand for *Ln* and O atoms, respectively.

$3s^2 3p^6 4s^2 3d^1$ and Y $4s^2 4p^6 5s^2 4d^1$ were treated as fully relaxed valence states. For the *f*-elements La, *f*-orbital was treated as valence orbital in the parameterized pseudo-potentials and the standard version was selected, whereas the semi-core *p*-states and *s*-states were treated as valence states, and hence the La $5s^2 5p^6 5d^1 6s^2$ states were treated as fully relaxed valence states. For Ce–Lu elements, *f*-electrons were partly kept frozen in the core, which is the standard model for the treatment of localized *f*-electrons, and the similar properties of the different lanthanides are linked to this core-like shell configuration. The number of *f*-electrons in the core equals the total number of valence electrons minus the formal valency 3. The compounds Eu_2O_3 and Yb_2O_3 were excluded from the present calculations since the trivalent pseudo-potentials of Eu and Yb elements are currently not available in the database distributed with the VASP package.

For the compounds with highly localized 3*d*, 4*f* or 5*f* electrons, the DFT, which is based on a static mean field description of the electron exchange and correlation, is not appropriate. Therefore, a modified scheme called DFT + *U* [47–52] is usually explored. In DFT + *U*, the Hamiltonian is parameterized by two parameters *U* and *J* that will favor integer occupation for the *f* states. Recently, a computational scheme, the so-called dynamical mean field theory (DMFT) [53,54] has been developed to handle this kind of systems. DMFT is a hybrid between a DFT and a model Hamiltonian approach. However, for the rare-earth sesquioxides Ln_2O_3, further investigations using the modified methods are needed to get more stable calculations. In the present paper, the results correspond to the traditional DFT method and the 4*f* states were partly kept frozen in the core to relieve the problem of the localized electrons.

The present calculations were performed at practically converged basis sets concerning the k-point sampling and kinetic energy cutoff based on the available computer resources. In particular, an $8 \times 8 \times 6$ gamma centered grids method [45] was employed to sample the Brillouin zone of all the *A*-Ln_2O_3 (hexagonal); the unit cell includes five atoms and the k-points number in the reciprocal space is 50. A $3 \times 3 \times 3$ Monkhorst–Pack net [55] was used to sample the Brillouin zone of all the *B*-type (monoclinic) sesquioxides; the unit cell includes 30 atoms and the k-points number in the reciprocal space is 10. The kinetic energy cutoff was set at 520 eV, which increases the cutoff energy of O by 30% compared with the default value set in the potential file. The computational parameters were carefully checked and a stable calculated result was obtained. Convergence tests concerning k-points and kinetic energy cutoff show that the total energies convergence is less than 2 meV/atom. The atomic geometry was optimized with Hellman–Feynman forces and conjugate gradient method [56]. When determining the equilibrium crystal structural parameters at absolute zero temperature and zero pressure, the total energy, E_{tot}, was minimized with respect to the volume (volume relaxation), the shape of the unite cell (cell external relaxation) and the position of the atoms within the cell (cell internal relaxation) fully. While when determining the transition pressure by analyzing the equation of state [57,58] of the oxides, the total energies under a series of prescribed volumes were calculated for each phase. To each unit cell volume, E_{tot} was minimized with respect to the shape of the unit cell and the position of the atoms within the cell. The process was terminated when the atomic force was less than 0.05 eV/Å.

3. Results and discussion

3.1. Equilibrium crystal structural parameters

The calculated crystal structural parameters and total energy of the two types of rare-earth sesquioxides Ln_2O_3, as well as the selected experimental structural data were compiled in Table 2 for the *A*-Ln_2O_3, and in Tables 3–5 for the *B*-Ln_2O_3, respectively. For the sake of brevity, only the variable lattice parameters and atomic internal parameters were presented. The volumes per formula unit of the polymorphic Ln_2O_3 at the ground state are shown in Figs. 2 and 3 for the *A*-Ln_2O_3 and *B*-Ln_2O_3, respectively, together with the critically assessed data [24] superimposed, although the direct comparison is not possible since the thermal expansion coefficients for most compounds are not available.

From Tables 2–5, Figs. 2 and 3, it is seen that the calculated lattice constants and volumes of unit cell agree well with the available experimental results and the critically assessed data, except Ce_2O_3, Pr_2O_3, and Nd_2O_3, for which the calculated volumes were overestimated about 4.0% and the modified DFT methods, such as DFT + *U* [47–52] and DMFT [53,54], are expected to improve the calculations further. The calculated atomic internal parameters are also close to the available experimental data. For *Ln* = La–Lu, with the increase of the atomic number, the ionic radius of rare-earth elements *Ln* [10] and the volumes of the Ln_2O_3 sesquioxides reflect the so-called "lanthanide contraction". For the same chemical constituent, the volume per formula of the *A*-type is smaller than its *B*-type, which implies that it is possible to transform the polymorphic compounds from the *B*-type to its *A*-type using high-pressure even around the room temperature under static [16–23] or shock compression [15,17].

3.2. Phase transition of the polymorphic Ln_2O_3 between the A- and B-type

The enthalpies of transition with respect to the transition of Ln_2O_3 from the *A*- to *B*-type at absolute zero temperature, zero pressure and without zero-point motion, $\Delta H_{tr,(A\to B)}$, were calculated according to Eq. (1):

$$\Delta H_{tr,(A\to B)} = E_{tot}(B) - E_{tot}(A), \quad (1)$$

The results are shown in Fig. 4, together with the critically assessed data [24] superimposed. It is seen that the current calculations agree quite well with the critically

Table 2
The calculated equilibrium crystal structural parameters and total energies of *A*-type Ln_2O_3 in comparison with the selected experimental data

Ln	Method	*a* (Å)	*c* (Å)	*V* (Å^3//Ln_2O_3)	$z_{Ln,2d}$	$z_{O1,2d}$	E_{tot} (eV/Ln_2O_3)	Reference
Sc	Calc.	3.3888	5.6624	56.33	0.2480	0.6479	−44.6351	
Y	Calc.	3.6582	5.9157	69.58	0.2497	0.6648	−45.2299	
La	Calc.	3.9379	6.1729	82.90	0.2472	0.6454	−41.9079	
	Expt.[a]	3.934	6.136	82.24	0.24604(7)	0.6464(5)		[59]
	Expt.	3.9381(3)	6.1361(6)	82.41	0.2467(2)	0.6470(2)		[40]
	Expt.	3.94	6.13	82.41	0.245(5)	0.645(5)		[60]
	Expt.	3.94	6.13	82.41	0.235	0.63		[61]
Ce	Calc.	3.9437	6.1908	83.38	0.2484	0.6454	−40.6376	
	Expt.	3.89100	6.05900	79.44	0.24543	0.6471		[62]
Pr	Calc.	3.8986	6.1354	80.76	0.2486	0.6447	−40.8945	
	Expt.	3.8589(1)	6.0131(2)	77.55	0.24630(5)	0.6555(8)		[63]
	Expt.	3.8577(3)	6.0120(6)	77.48				[64]
Nd	Calc.	3.8591	6.0899	78.54	0.2489	0.6447	−41.0803	
	Expt.	3.8272(1)	5.9910(2)	76.0	0.2473(3)	0.6464(3)		[65]
	Expt.	3.831	5.999	76.25	0.2462(3)	0.6466(3)		[66]
Pm	Calc.	3.8208	6.0393	76.35	0.2490	0.6449	−41.2939	
Sm	Calc.	3.7941	6.0114	74.94	0.2491	0.6449	−41.3363	
	Expt.	3.778	5.940	73.42				[16]
Eu	Calc.	–	–	–	–	–	–	
Gd	Calc.	3.7305	5.9386	71.45	0.2496	0.6453	−41.6172	
Tb	Calc.	3.7149	5.8576	70.01	0.2498	0.6464	−41.7047	
Dy	Calc.	3.6790	5.8766	68.88	0.2499	0.6454	−41.7398	
Ho	Calc.	3.6546	5.8488	67.65	0.2499	0.6460	−41.8004	
Er	Calc.	3.6338	5.8286	66.65	0.2502	0.6457	−41.8377	
Tm	Calc.	3.6099	5.7937	65.35	0.2502	0.6463	−41.7963	
Yb	Calc.	–	–	–	–	–	–	
Lu	Calc.	3.5643	5.7685	63.47	0.2504	0.6464	−41.9863	

[a]The number in parentheses in each case is the estimated error or the standard error, in units of the last decimal.

Table 3
The calculated lattice parameters and total energies of the *B*-type Ln_2O_3 in comparison with the selected experimental data

Ln	Method	*a* (Å)	*b* (Å)	*c* (Å)	*β* (deg)	V (Å^3//Ln_2O_3)	E_{tot} (eV/Ln_2O_3)	Reference
Sc	Calc.	13.3617	3.2166	8.0584	100.574	56.70	−44.9478	
Y	Calc.	14.1191	3.5174	8.6958	100.279	70.78	−45.3291	
La	Calc.	14.7541	3.8026	9.2223	100.123	84.85	−41.8576	
Ce	Calc.	14.7850	3.7946	9.2310	100.066	84.96	−40.6027	
Pr	Calc.	14.6489	3.7498	9.1350	100.062	82.33	−40.8744	
Nd	Calc.	14.5369	3.7097	9.0535	100.097	80.09	−41.0746	
Pm	Calc.	14.4185	3.6704	8.9643	100.113	77.82	−41.3025	
Sm	Calc.	14.3812	3.6352	8.9114	100.152	76.41	−41.3620	
	Expt.[a]	14.1975(9)	3.6273(3)	8.8561(5)	99.986(5)	74.86		[67]
	Expt.	14.177	3.627	8.845	99.98	74.66		[68]
	Expt.	14.177(10)	3.633(10)	8.847(10)	99.96(3)	74.80		[41]
Eu	Calc.	–	–	–	–		–	
	Expt.	14.1105(2)	3.6021(1)	8.8080(2)	100.037(1)	73.47		[69]
Gd	Calc.	14.1948	3.5658	8.7702	100.182	72.80	−41.6718	
Tb	Calc.	14.1298	3.5367	8.7155	100.211	71.42	−41.7655	
	Expt.	14.03(1)	3.536(5)	8.717(5)	100.10(5)	70.96		[70]
Dy	Calc.	14.0814	3.5104	8.6578	100.262	70.16	−41.8283	
Ho	Calc.	13.9914	3.4887	8.6101	100.266	68.90	−41.8883	
Er	Calc.	14.3812	3.6352	8.9114	100.278	67.77	−41.9627	
Tm	Calc.	13.8615	3.4335	8.4989	100.265	66.32	−41.9437	
Yb	Calc.	–	–	–	–		–	
Lu	Calc.	13.7431	3.3940	8.4180	100.307	64.36	−42.1671	

[a]The number in parentheses in each case is the estimated error or the standard error, in units of the last decimal.

Table 4
The calculated variable internal parameters of the element *Ln* in the *B*-type Ln_2O_3 in comparison with the selected experimental data

Ln	Method	$x_{Ln1,4i}$	$z_{Ln1,4i}$	$x_{Ln2,4i}$	$z_{Ln2,4i}$	$x_{Ln3,4i}$	$z_{Ln3,4i}$	Reference
Sc	Calc.	0.6353	0.4870	0.6958	0.1371	0.9695	0.1835	
Y	Calc.	0.6351	0.4880	0.6914	0.1374	0.9680	0.1858	
La	Calc.	0.6346	0.4923	0.6903	0.1382	0.9669	0.1883	
Ce	Calc.	0.6347	0.4902	0.6903	0.1377	0.9666	0.1890	
Pr	Calc.	0.6345	0.4900	0.6906	0.1379	0.9667	0.1885	
Nd	Calc.	0.6344	0.4899	0.6907	0.1377	0.9668	0.1885	
Pm	Calc.	0.6345	0.4895	0.6988	0.1376	0.9670	0.1883	
Sm	Calc.	0.6346	0.4892	0.6911	0.1378	0.9673	0.1873	
	Expt.[a]	0.63463(4)	0.49003(6)	0.68996(4)	0.13782(6)	0.96627(4)	0.18794(6)	[67]
	Expt.	0.6374	0.4897	0.6897	0.1376	0.9663	0.1876	[68]
	Expt.	0.6349	0.4905	0.6897	0.138	0.9663	0.1881	[41]
Eu	Calc.	–	–	–	–	–	–	
	Expt.	0.63740(1)	0.4897(2)	0.68972(1)	0.13760(2)	0.96635(1)	0.18763(2)	[69]
Gd	Calc.	0.6347	0.4885	0.6913	0.1376	0.9675	0.1867	
Tb	Calc.	0.6348	0.4881	0.6914	0.1375	0.9677	0.1864	
	Expt.	0.6349	0.4886	0.6901	0.1384	0.9666	0.1871	[70]
Dy	Calc.	0.6346	0.4883	0.6917	0.1379	0.9680	0.1860	
Ho	Calc.	0.6347	0.4879	0.6916	0.1371	0.9679	0.1859	
Er	Calc.	0.6348	0.4879	0.6914	0.1375	0.9680	0.1860	
Tm	Calc.	0.6351	0.4874	0.6917	0.1374	0.9680	0.1854	
Yb	Calc.	–	–	–	–	–	–	
Lu	Calc.	0.6351	0.4875	0.6917	0.1373	0.9681	0.18534	

[a]The number in parentheses in each case is the estimated error or the standard error, in units of the last decimal.

Table 5
The calculated variable internal parameters of the element O in the *B*-type Ln_2O_3 in comparison with the selected experimental data

Ln	Method	$x_{O1,4i}$	$z_{O1,4i}$	$x_{O2,4i}$	$z_{O2,4i}$	$x_{O3,4i}$	$z_{O3,4i}$	$x_{O4,4i}$	$z_{O4,4i}$	Reference
Sc	Calc.	0.1266	0.2794	0.8264	0.0344	0.7818	0.3787	0.4678	0.3411	
Y	Calc.	0.1281	0.2818	0.8255	0.0304	0.7933	0.3775	0.4711	0.3427	
La	Calc.	0.1281	0.2863	0.8240	0.0251	0.7995	0.3731	0.4742	0.3434	
Ce	Calc.	0.1292	0.2864	0.8244	0.0258	0.7986	0.3728	0.4742	0.3441	
Pr	Calc.	0.1291	0.2860	0.8245	0.0260	0.7984	0.3731	0.4740	0.3440	
Nd	Calc.	0.1292	0.2857	0.8246	0.0264	0.7982	0.3731	0.4738	0.3439	
Pm	Calc.	0.1290	0.2854	0.8248	0.0269	0.7979	0.3731	0.4735	0.3440	
Sm	Calc.	0.1288	0.2844	0.8249	0.0280	0.7965	0.3746	0.4728	0.3436	
	Expt.[a]	0.1289(6)	0.2864(8)	0.8250(6)	0.0265(8)	0.7984(6)	0.3738(9)	0.4741(6)	0.3438(8)	[67]
	Expt.	0.1291	0.2855	0.8248	0.0267	0.7961	0.3732	0.4734	0.3431	[68]
	Expt.	0.128	0.286	0.824	0.027	0.799	0.374	0.469	0.344	[41]
Eu	Calc.	–	–	–	–	–	–	–	–	
	Expt.	0.1291(2)	0.2855(3)	0.8248(2)	0.0267(3)	0.7961(3)	0.3732(4)	0.4734(2)	0.3431(3)	[69]
Gd	Calc.	0.1284	0.2831	0.8250	0.0291	0.7952	0.3760	0.4721	0.3433	
Tb	Calc.	0.1383	0.2823	0.8251	0.0297	0.7943	0.3769	0.4716	0.3431	
	Expt.	0.128	0.276	0.827	0.024	0.793	0.373	0.478	0.335	[70]
Dy	Calc.	0.1279	0.2822	0.8253	0.0302	0.7942	0.3771	0.4713	0.3431	
Ho	Calc.	0.1278	0.2815	0.8254	0.0302	0.7935	0.3768	0.4711	0.3430	
Er	Calc.	0.1277	0.2818	0.8254	0.0303	0.7936	0.3772	0.4711	0.3429	
Tm	Calc.	0.1277	0.2813	0.8255	0.0310	0.7930	0.3773	0.4703	0.3427	
Yb	Calc.	–	–	–	–	–	–	–	–	
Lu	Calc.	0.12760	0.28122	0.8257	0.0312	0.7929	0.3774	0.4699	0.3425	

[a]The number in parentheses in each case is the estimated error or the standard error, in units of the last decimal.

assessed data if we ignore the heat content difference for the phase transition at 0 k and at definite temperature due to the heat capacity data for *A*- and *B*-Ln_2O_3 compounds are not available simultaneously. From La to Nd, the *A*-type is more stable than its *B*-type. The results in Fig. 4 from both our *ab initio* calculation and the critical assessment show that, in general, with the increase of the Ln^{3+}-cation radius [10], the polymorphic structures of Ln_2O_3 have a degenerative tendency.

The quantitative relationships of the total energies versus volumes were fitted with the empirical third-order Birch–Murnaghan equation of state [57,58] to obtain an

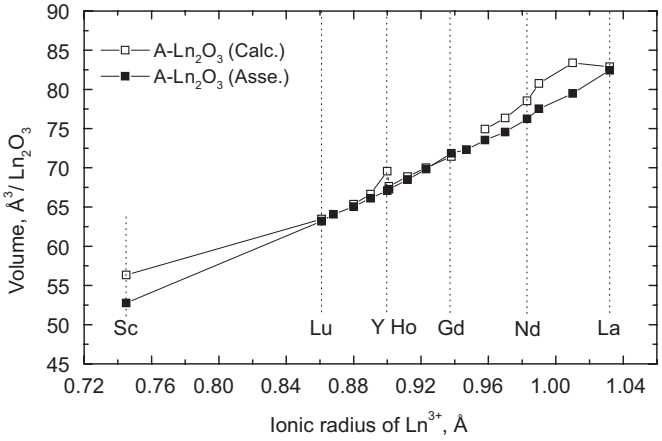

Fig. 2. The calculated volume per formula of the *A*-Ln_2O_3 sesquioxides in comparison with the critically assessed data [24].

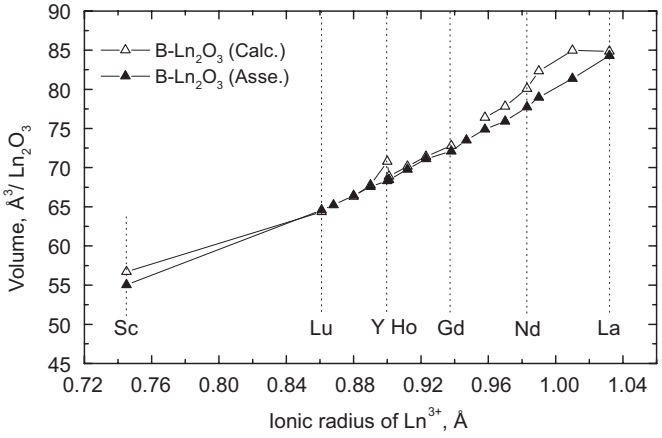

Fig. 3. The calculated volume per formula of the *B*-Ln_2O_3 sesquioxides in comparison with the critically assessed data [24].

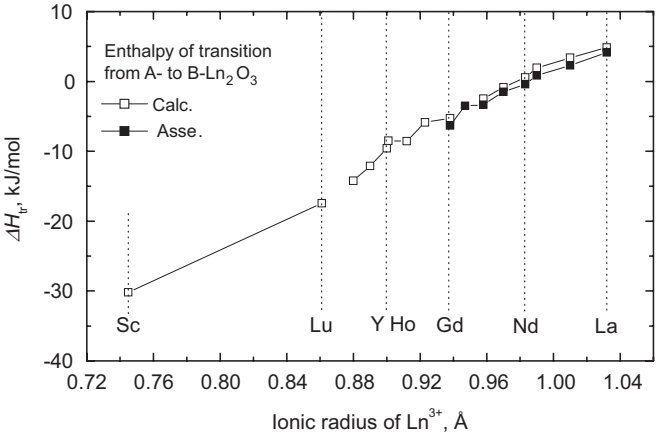

Fig. 4. The calculated enthalpy of transition with respect to the transition of Ln_2O_3 from its *A*- to *B*-type together with the critically assessed data [24] superimposed.

analytical interpolation of the computed points. And the properties such as equilibrium volume and total energy, bulk modulus, and transition pressure can be derived. The room-temperature third-order Birch–Murnaghan isothermal equation of state [57,58] is given by

$$E(V) = E_0 + \frac{9V_0B_0}{16}\left[\left(\frac{V_0}{V}\right)^{2/3} - 1\right]^3 B_0' + \left[\left(\frac{V_0}{V}\right)^{2/3} - 1\right]^2\left[6 - 4\left(\frac{V_0}{V}\right)^{2/3}\right], \quad (2)$$

where E_0 and V_0 are the total energy and volume per Ln_2O_3 formula unit, respectively, and B_0 is the bulk modulus. E_0, V_0, and B_0 are corresponding to the zero-pressure value. B' is the bulk modulus pressure derivative, which is found to change little with pressure. B'_0 is the bulk modulus pressure derivative at P=0. Generally, Many substances have a fairly constant B' and B'_0 as $B' = B'_0 = 3.5$ [57,58]. In mathematics, B'_0 can be also obtained by fitting the room-temperature third-order Birch–Murnaghan isothermal equation of state [57,58], but the more parameters to fit, the more complexity and uncertainty involved in the fitting procedure. Referring to the experimental experience and our test results, here we also fixed $B' = B'_0 = 3.5$.

The results for the representative Sm_2O_3 are shown in Fig. 5, where the plotted symbols representing the computed values and the curves representing the fitted results. The transition pressure was obtained by calculating the common tangent slope of the two fitted curves. It is seen that the calculated result of the transition pressure with respect to the transition of Sm_2O_3 from its *B*- to *A*-type in Fig. 5 locates in the range of the experimental data, which the present result is $P_{tr} = 3.340$ GPa and the experimental value is from 3.2 to 3.9 GPa [16].

The fitted equilibrium volume and total energy recurred the data determined by directly optimizing the geometry fully. The bulk modulii of the rare-earth sesquioxides Ln_2O_3 obtained by fitting E–V data based-on the empirical third-order Birch–Murnaghan equation of state are shown in Fig. 6. It is seen that the bulk modulus of Ln_2O_3

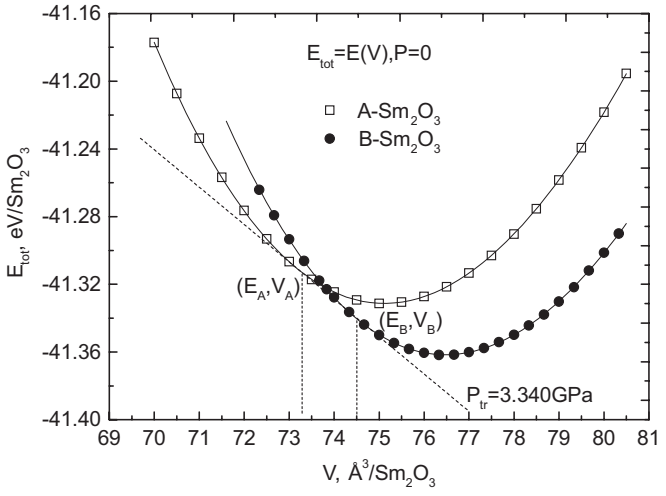

Fig. 5. The total energy vs. volume (per Sm_2O_3 formula unit) for the *A*- and *B*-type Sm_2O_3.

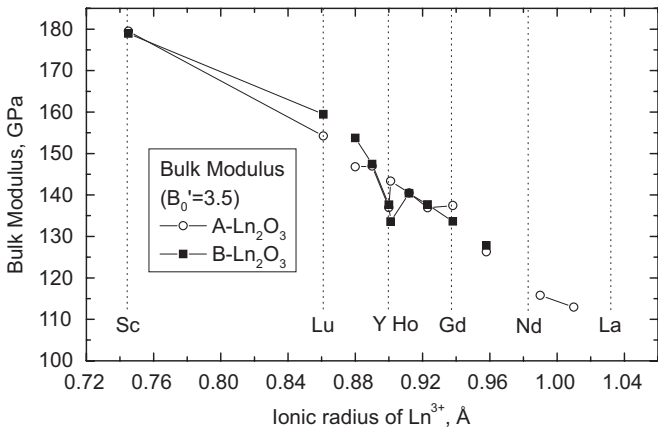

Fig. 6. The calculated bulk modulus of the rare-earth sesquioxide Ln_2O_3.

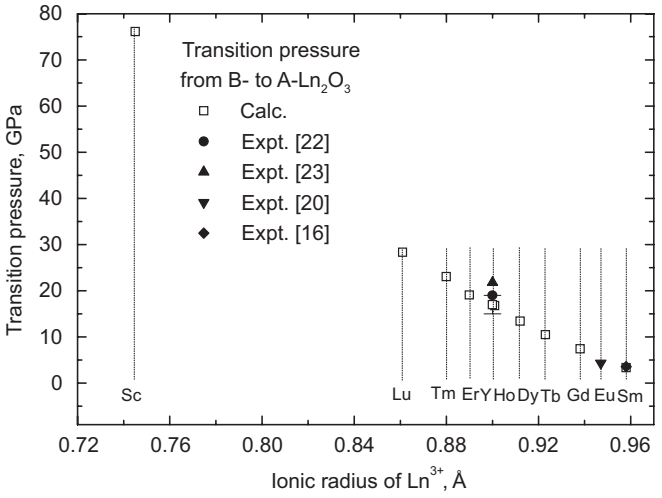

Fig. 7. The calculated transition pressure with respect to the transition of the Ln_2O_3 from its *B*- to *A*-type together with the available experimental data superimposed.

decreases with the increase of the Ln^{3+}-cation radius, and the difference between the *A*- and *B*-type is considerably small.

The calculated transition pressures with respect to the transition of Ln_2O_3 from the *B*-type to *A*-type are shown in Fig. 7, together with the available experimental data superimposed. The present calculated results show that it is not possible to realize the $B\text{-}Ln_2O_3 \rightarrow A\text{-}Ln_2O_3$ transition with *Ln* from La–Nd using the pressure-induced phase transition method because the transition pressures are negative. From Fig. 7, it is seen that the calculated values reasonably agree with the available experimental results, and valuable data are afforded to the compounds, for which no experimental data are available. The transition pressures decrease with the increase of the Ln^{3+}-cation radius, which also reflects the degenerative tendency.

4. Conclusions

The structural and energetic data of the polymorphic rare-earth sesquioxides Ln_2O_3 (Ln = La–Lu, Y, and Sc) with *A*-type (hexagonal) and *B*-type (monoclinic) configurations were computed systematically for the first time using *ab initio* calculations based on density function theory (DFT) and PAW pseudo-potentials method. The volumes of the unit cells and the relative lattice stabilities between *A*- and *B*-type agree well with the critically assessed data. The *ab initio* calculation is a powerful tool to produce valuable and accurate data for the interested compounds. A self-consistent database comprising the crystal structural parameters and thermodynamic properties was established. With the increase of the atomic number, the ionic radius of rare-earth elements *Ln*, as well as the volume of the sesquioxides Ln_2O_3 (Ln = La–Lu) reflect the so-called "lanthanide contraction". With the increase of the Ln^{3+}-cation radius, the bulk modulus of Ln_2O_3 decreases and the polymorphic structures show a degenerative tendency since the absolute enthalpies of transition and the transition pressures with respect to the transition from the *B*-type to their polymorphic *A*-type become smaller and smaller. However, further efforts are needed to better understand the highly localized 4*f* electrons and the potential parameterization of Eu_2O_3 and Yb_2O_3, as well as analyze the equation of state of the Ln_2O_3 (where Ln = La–Pm).

Acknowledgments

The *ab initio* calculations were performed in Max-Planck Institute for Metals Research, and Dr. Bo Wu gratefully acknowledges the Scholarship provided by Max-Planck-Society and the Science Foundations in Fuzhou University (Projects No.: 826212, 2007-XQ-03, and 2007F3045). The authors thank Dr. Chong Wang for the helpful discussions.

References

[1] G.M. Qiu, M. Zhang, L.X. Zhou, X.S. Chen, H.Y. Chen, C.H. Yan, H. Okamoto, J. Rare Earths 21 (1) (2003) 37–41.
[2] Z.H. Ma, J.F. Qiu, J. Rare Earths 22 (special issue) (2004) 287–294.
[3] X.Q. Cao, J. Mater. Sci. Technol. 23 (1) (2007) 15–35.
[4] K. Nouneh, A.H. Reshak, S. Auluck, I.V. Kityk, R. Viennois, S. Benet, S. Charar, J. Alloys Compd. 437 (2007) 39–46.
[5] Un Sik Seo, USA Patent 6428598, 1991.
[6] K.G. Mu, W.J. Zhang, J.Y. Cui, F.S. Zhang, L. Hu, J. Rare Earths 22 (3) (2004) 315–318.
[7] J.C. Wang, J. Yang, X.S. Liu, J. Rare Earths 22 (Special issue) (2004) 313–316.
[8] G. Brauer, in: L. Eyring (Ed.), Progress in the Science and Technology of the Rare Earths, Vol. 3, Pergamon Press, Oxford, 1968 p. 434.
[9] C.E. Holley Jr., E.J. Huber Jr., F.B. Baker, in: L. Eyring (Ed.), Progress in the Science and Technology of the Rare Earths, vol. 3, Oxford, Pergamon Press, 1968, p. 343.
[10] R.D. Shannon, Acta Crystallogr. A 32 (1976) 751–767.
[11] R.G. Haire, L. Eyring, in: K.A. Gschneidner Jr., L. Eyring, G.R. Chopping, G.R. Lander (Eds.), Handbook on the Physics and Chemistry of the Rare Earths, vol. 18. Lanthanides/Actinides: Chemistry, Elsevier Science BV, Amsterdam, 1994, p. 413.
[12] A.I. Kriklya, Powder Metall. Met. Ceram. 38 (1999) 274–277.
[13] E.H.P. Cordfunke, R.J.M. Konings, Thermochim. Acta 375 (1–2) (2001) 65–79.

[14] J.B. Gruber, B.H. Justice, E.F. Westrum Jr., B. Zandi, J. Chem. Thermodyn. 34 (2002) 457–473.
[15] J.Q. Sawyer, B.G. Hyde, L. Eyring, Inorg. Chem. 4 (1965) 426–427.
[16] T. Atou, K. Kusaba, Y. Tsuchida, W. Utsumi, T. Yagi, Y. Syono, Mater. Res. Bull. 24 (1989) 1171–1176.
[17] T. Atou, K. Kusaba, K. Fukuoka, M. Kikuchi, Y. Syono, J. Solid State Chem. 89 (1990) 378–384.
[18] G. Chen, N.A. Stump, R.G. Harie, J.R. Peterson, J. Alloys Compd. 181 (1992) 503–509.
[19] G. Chen, N.A. Stump, R.G. Harie, J.B. Burns, J.R. Peterson, High Pressure Res. 12 (1994) 83–90.
[20] G. Chen, J.R. Peterson, K.E. Brister, J. Solid State Chem. 111 (1994) 437–439.
[21] C. Meyer, J.P. Sanchez, J. Thomasson, J.P. Itie, Phys. Rev. B 51 (1995) 12187–12193.
[22] E. Husson, C. Proust, P. Gillet, J.P. Itie, Mater. Res. Bull. 34 (1999) 2085–2092.
[23] Y.M. Ma, H.A. Ma, Y.W. Pan, Q.L. Cui, B.B. Liu, T. Cui, G.T. Zhou, J. Liu, L.J. Wang, He Jishu/Nucl. Tech. 25 (2002) 841–844 (in Chinese).
[24] M. Zinkevich, Prog. Mater. Sci. 52 (2007) 597–647.
[25] P. Hohenberg, W. Kohn, Phys. Rev. 136 (3B) (1964) B864–B871.
[26] C. Colinet, Intermetallics 11 (2003) 1095–1102.
[27] H.J.F. Jansen, A.J. Freeman, Phys. Rev. B 30 (1984) 561–569.
[28] P.E. Blöchl, Phys. Rev. B 50 (1994) 17953–17979.
[29] G. Kresse, J. Joubert, Phys. Rev. B 59 (1999) 1758–1775.
[30] W. Kohn, L.J. Sham, Phys. Rev. 140 (1965) A1133–A1138.
[31] J.P. Perdew, Y. Wang, Phys. Rev. B 45 (1992) 13244–13249.
[32] J.P. Perdew, K. Burke, M. Ernzerhof, Phys. Rev. Lett. 77 (1996) 3865–3868.
[33] J.P. Perdew, K. Burke, M. Ernzerhof, Phys. Rev. Lett. 78 (1997) 1396.
[34] N. Hirosaki, S. Ogata, C. Kocer, J. Alloys Compd. 351 (2003) 31–34.
[35] A. Kuwabara, I. Tanaka, J. Phys. Chem. B 108 (26) (2004) 9168–9172.
[36] J.M. Pruneda, E. Artacho, Phys. Rev. B 72 (2005) 085107.
[37] L. Petit, A. Svane, Z. Szotek, W.M. Temmerman, Phys. Rev. B 72 (2005) 205118.
[38] B. Wu, M. Zinkevich, Ch. Wang, F. Aldinger, Rare Metals 25 (5) (2006) 549–555.
[39] B. Wu, M. Zinkevich, F. Aldinger, W.Q. Zhang, J. Phys. Chem. Solid 68 (2007) 570–575.
[40] P. Aldebert, J.P. Traverse, Mater. Res. Bull. 14 (1979) 303–323.
[41] D.T. Cromer, J. Phys. Chem. 61 (1957) 753.
[42] G. Kresse, J. Hafner, J. Phys.: Condens. Matter 6 (1994) 8245–8257.
[43] G. Kresse, J. Furthmüller, Comput. Mater. Sci. 6 (1996) 15–50.
[44] G. Kresse, J. Furthmüller, Phys. Rev. B 54 (1996) 11169–11186.
[45] G. Kresse, VASP, Vienna Ab-initio Simulation Package, 〈cms.mpi.univie.ac.at/vasp/〉.
[46] N.E. Holden, T. Coplen, Chem. Int. 26 (1) (2004) 8.
[47] V.I. Anisimov, J. Zaanen, O.K. Andersen, Phys. Rev. B 44 (1991) 943–954.
[48] V.I. Anisimov, F. Aryasetiawan, A.I. Liechtenstein, J. Phys.: Condens. Matter 9 (1997) 767–808.
[49] S.L. Dudarev, G.A. Botton, S.Y. Savrasov, C.J. Humphreys, A.P. Sutton, Phys. Rev. B 57 (1998) 1505–1509.
[50] A. Rohrbach, J. Hafner, G. Kresse, J. Phys.: Condens. Matter 15 (2003) 979–996.
[51] M. Cococcioni, S. de Gironcoli, Phys. Rev. B 71 (2005) 035105.
[52] L. Wang, T. Maxisch, G. Ceder, Phys. Rev. B 73 (2006) 195107.
[53] A. Georges, G. Kotliar, W. Krauth, M.J. Rozenberg, Rev. Mod. Phys. 68 (1996) 13–125.
[54] G. Kotliar, D. Vollhardt, Phys. Today 57 (2004) 53–59.
[55] H.J. Monkhorst, J.D. Pack, Phys. Rev. B 13 (1976) 5188–5192.
[56] M.P. Teter, M.C. Payne, D.C. Allan, Phys. Rev. B 40 (1989) 12255–12263.
[57] F.D. Murnaghan, Proc. Natl. Acad. Sci. USA 30 (1944) 244–247.
[58] F. Birch, Phys. Rev. 71 (1947) 809–824.
[59] G. Schiller, Dissertation, Universitaet Karlsruhe, Karlsruhe, Germany, 1985, p. 1.
[60] W.C. Koehler, E.O. Wollan, Acta Crystallogr. 6 (1953) 741–742.
[61] L. Pauling, Z. Kristallogr. Kristallgeom. Kristallphys. Kristallchem. 69 (1928) 415–421.
[62] H. Baernighausen, G. Schiller, J. Less Common Met. 110 (1985) 385–390.
[63] O. Greis, R. Ziel, B. Breidenstein, A. Haase, T. Petzel, J. Alloys Compd. 216 (1994) 255–258.
[64] R. Wolf, R. Hoppe, Z. Anorg. Allg. Chem. 529 (1985) 61–64.
[65] M. Faucher, J. Pannetier, Y. Charreire, P. Caro, Acta Crystallogr. B 38 (1982) 344–346.
[66] J.X. Boucherle, J. Schweizer, Acta Crystallogr. B 31 (1975) 2745–2746.
[67] T. Schleid, G. Meyer, J. Less Common Met. 149 (1989) 73–80.
[68] C. Boulesteix, B. Pardo, P.E. Caro, M. Gasgnier, C.H. la Blanchetais, Acta Crystallogr. B 27 (1971) 216–219.
[69] H.L. Yakel, Acta Crystallogr. B 35 (1979) 564–569.
[70] E. Hubbert-Paletta, H. Mueller-Buschbaum, Z. Anorg. Allg. Chem. 363 (1968) 145–150.